Crazes in diluted entanglement networks of polystyrene

ARTICLE *in* MACROMOLECULES · JULY 1986

Impact Factor: 5.8 · DOI: 10.1021/ma00161a040

4 AUTHORS, INCLUDING:

Arnold Chang-Mou Yang
National Tsing Hua University
71 PUBLICATIONS **690** CITATIONS
SEE PROFILE

S. Leigh Phoenix
Cornell University
136 PUBLICATIONS **4,182** CITATIONS
SEE PROFILE

Crazes in Diluted Entanglement Networks of Polystyrene

Arnold C.-M. Yang and Edward J. Kramer*

Department of Materials Science and Engineering and the Materials Science Center, Cornell University, Ithaca, New York 14853

Chia C. Kuo and S. Leigh Phoenix

Department of Mechanical and Aerospace Engineering and the Materials Science Center, Cornell University, Ithaca, New York 14853. *Received January 6, 1986*

ABSTRACT: In blends of high molecular weight polystyrene (PS) (M_w = 1 800 000) with low molecular weight PS (M_w = 2000) craze microstructure and fibril stability change dramatically with composition. Because the low molecular weight PS is too short to form effective entanglements, crazes become increasingly fragile as the concentration χ of the high molecular weight component decreases, and virtually no stable crazes are observed below χ = 0.3. The craze fibril extension ratio λ_{craze} is measured with optical microdensitometry of transmission electron microscope image plates. As χ decreases from 1.0 to 0.5, λ_{craze} increases approximately as λ_{max}, the maximum extension ratio of a single strand in the entanglement network, but for $\chi < 0.5$, λ_{craze} becomes significantly greater than λ_{max}. Average craze fibril diameters D and spacings D_0 are measured by low-angle electron diffraction (LAED). The craze fibril diameter D is approximately constant whereas the fibril spacing D_0 increases modestly as χ decreases. Craze fibril stability, as measured by the median strain ϵ_b for craze breakdown, decreases almost linearly with χ and approaches zero at χ = 0.3. Dust particle inclusions significantly reduce craze fibril stability but do not change the shape of the ϵ_b vs. χ curves. Various other molecular weights, M = 600, 10 000, 17 500, 20 400, 37 000, 50 000, and 110 000, were used as the low molecular weight component at χ = 0.3 to investigate the effect of diluent molecular weight. While the craze fibril stability is still close to zero in the region $2000 \le M \le 37\,000$, it rises sharply in the region between 37 000 and 110 000. For the case of M = 600, however, the T_g of the blends with $\chi \le 0.5$ is at or below room temperature; no crazes or local deformation zones form in these blends. From the measured structural parameters, D and D_0, one can calculate the effective number of entangled strands n_e in each fibril (after the entanglement loss during fibrillation). While no average molecular weight can correlate the fibril stability of the monodisperse PS's and the blends, a plot of fibril stability vs. n_e produces superposition of all the data on a single curve. Craze fibril stability was found to increase exponentially with n_e, in accord with a model which assumes that the n_e strands must independently break or disentangle for craze breakdown to occur.

Introduction

The origin of brittle fracture in many glassy polymers is the formation and breakdown of crazes, local microdeformation zones with fibrillar structure.[1-4] The fibrils in the crazes are drawn from the strain-softened polymer bulk at a constant value of fibril extension ratio λ_{craze} ($\approx$4 for polystyrene (PS)) and are load-bearing.[4,5] The first step, and usually the slowest, of the mechanical failure process in this class of materials is the breakdown of the individual fibrils to form a large void in the craze.[6,7] When the void grows to a critical size, it propagates as a crack, causing catastrophic fracture. The strength of polymer glasses is mirrored by the stability of the individual fibrils.[8,9] We define the craze fibril stability as the plastic strain due to crazing that can be achieved at the onset of fibril breakdown to form a large void.

To understand and control the craze fibril stability, we must first understand the mechanisms involved in fibril formation and the molecular factors governing fibril breakdown. A model concerning the entanglement loss after craze fibrillation has been proposed previously.[4,8] We present in this paper the experimental results on a wide range of craze microstructures from which several important microscopic parameters can be obtained and used to correlate the craze fibril stability.

The second major purpose of this paper is to explore the effects[10] on craze fibril structure and stability of dilution of high molecular weight polymer with a short-chain species. Since the high and low molecular weight polystyrenes do not phase separate, fully compatible blends may be produced in which the entanglement network is diluted. The dilution has a pronounced influence on both craze fibril structure and stability. This result has important implications for fracture properties of the products fabricated from broad molecular weight distribution polymers to which a low molecular weight "tail" is added to improve processibility. With the knowledge of the diluent effects of these short-chain species on craze fibril stability a blending law for fracture properties may eventually be formulated.

Experimental Procedures

Monodisperse polystyrenes (M_w/M_n < 1.3) purchased from Pressure Chemical Co. were used throughout the experiment. For the initial experiments, high molecular weight PS (M_w = 1 800 000) and low molecular weight PS (M_w = 2000) were dissolved in toluene to form a solution with a fixed volume fraction χ of the 1 800 000 molecular weight PS. In subsequent experiments, molecular weights of 600, 10 000, 17 500, 20 400, 37 000, 50 000, and 1 000 000 were also used as the low molecular weight component to examine the effect of the molecular weight of the "diluent". Films of the PS blends were prepared by drawing glass slides from the above solutions at a constant speed. The thickness of the film was measured with a Zeiss interference microscope and was held constant at 0.4 μm by adjusting the polymer concentration of the solution. After the toluene evaporated, the PS blend film was floated off the glass slide onto the surface of a water bath and picked up on a ductile copper grid. The bars of the grid were previously coated with a thin layer of PS by dipping it into the PS solution. A short exposure to toluene vapor bonded the PS film to the copper grid and removed all the slack in the film.[11] When the copper grid was plastically deformed, the grid bars transferred the strain to the supported PS film. The grid subdivided the PS film into a large number ($\approx$40) of independent film squares, each of which had a linear dimension of approximately 1 mm. To remove residual solvent, all specimens were stored under vacuum at room temperature for 35 h before crazing.

The crazing and fibril breakdown process were studied by deforming the grids in tension at a constant slow strain rate. A deformed film square of interest could then be cut from the copper grid and examined in the transmission electron microscope (TEM). The first task was to determine quantitative information about the craze microstructure. A starter "crack" (a slot of dimensions

0024-9297/86/2219-2020$01.50/0

120 μm × 10 μm) with its length normal to the tensile axis was burned into the center of several film squares, using the intensely focused electron beam of an electron microprobe.[12] Wide crazes could then be grown from these starter cracks for microstructure determination. Each specimen was deformed at the low strain rate 5×10^{-7} s^{-1} to a strain of 2%, except the fragile $\chi = 0.4$ and $\chi = 0.3$ blends, where smaller strains were used. The crazes were examined by TEM immediately after straining to minimize fibril coalescence.[13]

For quantitative information of craze fibril structure, optical microdensitometry[5] of the TEM image plate and low-angle electron diffraction (LAED)[13,14] were used respectively to determine the craze fibril extension ratio λ_{craze} and the average fibril diameter D and spacing D_0. The optical densities of the craze (ϕ_c), the undeformed PS film (ϕ_f), and the starter crack (ϕ_h) were measured by using a microdensitometer to scan appropriate areas on the TEM negatives. The craze fibril extension ratio λ_{craze} was determined from[5]

$$\lambda_{craze} = [1 - \ln (\phi_c/\phi_f)/\ln (\phi_h/\phi_f)]^{-1} \quad (1)$$

LAED was carried out by using the JEOL 200CX electron microscope operating at its longest camera length, 62.6 m. The craze LAED pattern was scanned by a microdensitometer to sum the diffracted intensity along the fibril axis (the y axis), producing a slit-smeared scattering curve $i(s)$. s is the scattering vector normal to the fibril axis (the x axis) defined as $s = 2\theta/\lambda$, in which θ is the scattering angle and λ the electron wavelength. The average craze fibril diameter D was determined from the high-angle region of the diffraction curve using Porod's law,[15-17] and the average fibril spacing D_0 was obtained from the relationship[4]

$$D_0 = (\lambda_{craze})^{1/2} D \quad (2)$$

which assumes constant polymer volume during fibril drawing. Since the craze fibrils have a broad distribution of fibril size and the diffraction intensity increases with the fourth power of the fibril diameter,[16] the "long spacing" of craze fibrils, s_{max}^{-1}, obtained from the inverse of the maximum of $i(s)$, s_{max}, is always larger than the fibril spacing D_0 obtained from eq 2.

The second task was to deform several grids in tension while monitoring with an optical microscope the number fraction of film squares which had crazed, undergone local craze fibril breakdown, and catastrophically fractured, respectively, as a function of strain during the test. (The procedures and mathematical methods parallel those in our earlier study,[9] and we refer the reader to that work for details.) From plots of these number fractions the median strains for craze initiation ϵ_c, for craze fibril breakdown ϵ_b, and for catastrophic fracture ϵ_f were determined. (The median strain corresponds to the strain at which the specified event has occurred in half the film squares.) The plastic strain due to crazing before fibril breakdown, $\epsilon_b - \epsilon_c$, is taken as a measure of craze fibril stability.

Dust particle inclusions in the PS films were found to have important effects on craze fibril stability; therefore a procedure to prepare clean samples[9] was followed. A porous ceramic filter with an average pore size 10 μm was used to remove dust particles from the solutions prior to casting. No molecular weight degradation due to filtering was measured by viscometry. The filtration and the sample preparation were carried out in a class 10 clean hood in a clean room of the National Research and Resource Facility for Submicron Structure (NRRFSS), Knight Laboratory, Cornell University. Thus we were able to compare results for both unfiltered and filtered ("ultraclean"[9]) specimens.

Experimental Results

The addition of the 2000 molecular weight short chains to the high molecular weight PS decreases the craze fibril stability. At a strain rate of 5×10^{-7} s^{-1}, a film square of undiluted PS can typically endure a tensile strain of greater than 25% before catastrophic fracture, whereas blends with $\chi = 0.3$ suffer brittle failure at a low strain of 0.8%, as shown in Figure 1. For $\chi \leq 0.2$, the blends were so fragile that usually no stable crazes were observed prior to crack propagation.

Craze microstructure noticeably changes as the concentration of the low molecular weight ($M_w = 2000$) PS increases. The TEM micrographs of the crazes in the PS blends displayed in Figure 2 show, as χ decreases, a clear decrease in the fibril volume fraction and an increase in the width of the midrib, the region of high fibril extension ratio in the center of the craze. The midrib contains few cross-tie fibrils, small fibrils that span laterally from one major load-bearing fibril to the next. Direct measurement of the midrib width from the TEM micrographs reveals that the midrib width increases linearly with the concentration of the low molecular weight component; these results are given in Table I. Ultimately at $\chi = 0.3$, there is no distinction between the midrib and the ordinary fibrils; no cross-tie fibrils are present anywhere in the craze.

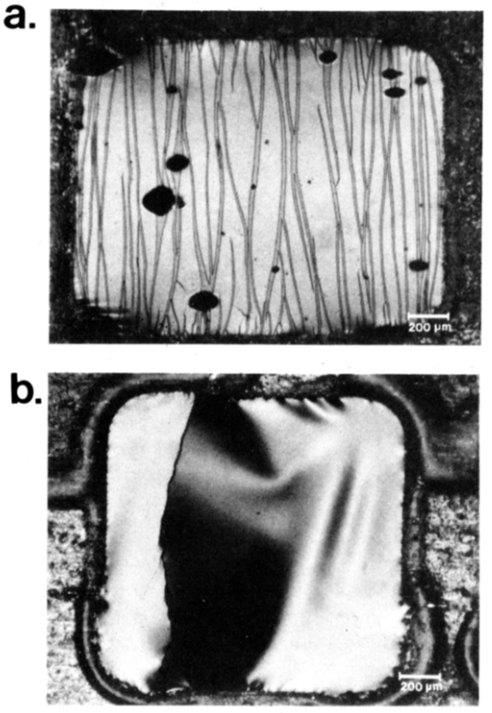

Figure 1. Optical micrographs of the craze and crack morphology in a film square deformed at a strain rate of 5×10^{-7} s^{-1} in (a) an 1 800 000 molecular weight PS ($\chi = 1.0$, strain = 26.5%) and (b) a PS blend (2000 + 1 800 000) ($\chi = 0.3$, strain = 0.6%).

Table I
Craze Fibril Long Spacings and Midrib Widths in the Diluted Polystyrenes

χ (1 800 000 wt fract)	long spacing s_{max}^{-1}, nm	midrib width, μm
1.0	27.0	0.12
0.9	31.0	0.16
0.7	34.2	0.25
0.5	48.0	0.32
0.4	47.0	0.36

The craze fibril extension ratios λ_{craze} of PS blends (2000 + 1 800 000) are shown in Figure 3. λ_{craze} is observed to increase as the high molecular weight concentration χ decreases. Also shown in the figure are the values of the maximum single-strand extension ratio λ_{max} predicted for the diluted blends. This extension ratio is defined as $\lambda_{max} = l_e/d$, where l_e is the chain contour length and d is the root-mean-square end-to-end distance between nodes in an entanglement network whose strands have molecular weight M_e, the entanglement molecular weight.[18] For no chain scission or disentanglement, λ_{max} is the maximum extension ratio of a single strand of which l_e is the contour chain length.[4,19] For a network of such strands,[4] however, the maximum extension ratio is approximately $3^{1/2} \lambda_{max}$. We can consider the blend as a solid solution of which the

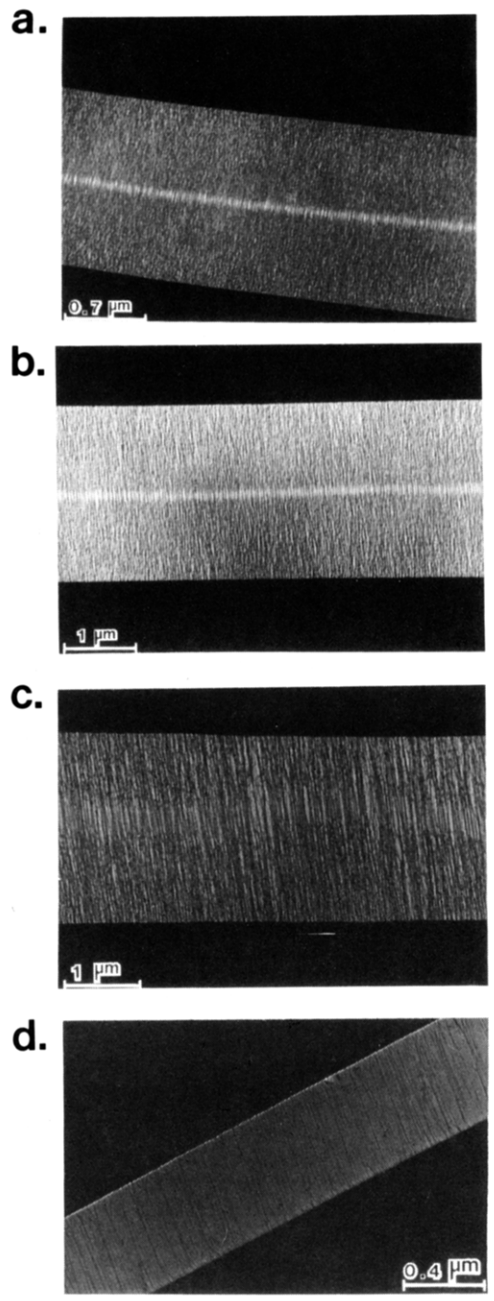

Figure 2. TEM micrographs of the crazes in the PS blends (2000 + 1 800 000): (a) $\chi = 1.0$; (b) $\chi = 0.7$; (c) $\chi = 0.5$; (d) $\chi = 0.3$.

high molecular weight PS is the solute and the low molecular weight PS the solvent. In a solution like this, the chain contour length l_e scales as $1/\chi$, while the entanglement mesh size d scales as $\chi^{-5/8}$ for good solution, and as $\chi^{-1/2}$ for Θ solution.[20] Therefore, λ_{max} for the PS blend is given by

$$\lambda_{max}(\chi) = \lambda_{max}(\chi = 1)/\chi^{3/8} \qquad \text{(good solution)} \qquad (3a)$$

and

$$\lambda_{max}(\chi) = \lambda_{max}(\chi = 1)/\chi^{1/2} \qquad (\Theta \text{ solution}) \qquad (3b)$$

where $\lambda_{max}(\chi = 1)$ is equal to 4.2, calculated from $l_e = 40$ nm and $d = 9.6$ nm for PS. For the blends where $0.5 \leq \chi \leq 1.0$, the average λ_{craze} closely follows the value of λ_{max}, which increases modestly in this region, but for the blends of $0.3 \leq \chi < 0.5$ the average λ_{craze} increases sharply and is significantly higher than λ_{max} predicted from the network model. The low molecular weight solvents act like diluents to dilute the entanglement network of the high molecular

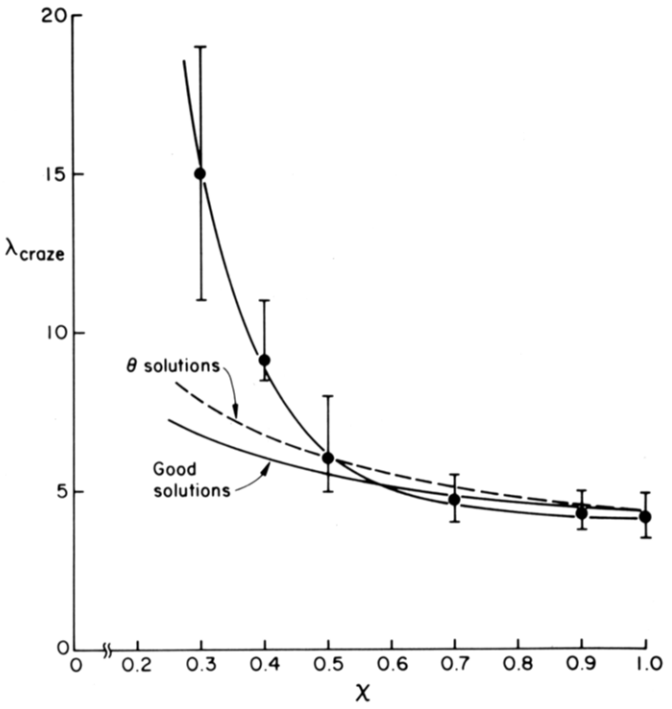

Figure 3. Craze fibril extension ratio λ_{craze}, measured by optical microdensitometry of TEM images, as a function of the high molecular weight fraction χ in the PS blend. The solid and dashed lines are λ_{max}, computed by assuming the 2000 molecular weight PS is a good solvent and a Θ solvent (eq 3), respectively, for high molecular weight PS.

weight solutes. On the basis of de Gennes' scaling argument,[20] the blends of (2000 + 1 800 000) fall in the category of good solutions, although screening effects[20] may substantially cancel the excluded volume effect in the high-χ range, where we observe stable crazes.[21] However, the large scatter in the measured λ_{craze} values makes it impossible to distinguish between the behavior of a good or Θ solution.

Low-angle electron diffraction (LAED) patterns of the crazes grown from the "crack" tip are shown in Figure 4 for the PS blends $\chi > 0.3$. For $\chi = 0.3$, the crazes which are stable under the electron beam are not wide enough to produce a LAED pattern for quantitative analysis. The streaks along the x axis (parallel to craze length) are due to the scattering from the craze fibrils. The narrow sharp streaks along the y axis (parallel to the tensile stress) result from electron refraction at the craze–bulk interfaces.[14] Figure 5 shows the corresponding $i(s)$ curve for each pattern in Figure 4. The long spacing s_{max}^{-1} measured from the maximum of $i(s)$ increases modestly with decreasing χ, as shown in Table I. The typical exposure time for LAED is 3–10 min and the effects of electron damage are minimal as evidenced from the comparison between two LAED patterns taken one after the other from the same region in the craze. The average fibril diameter D is almost constant in the range $0.4 \leq \chi \leq 1.0$, at a value approximately 10 nm. The fibril diameter D of the crazes in the blend $\chi = 0.3$ can be roughly estimated from the TEM micrographs since the craze fibril density is so low in this highly diluted blend. The average fibril spacings D_0 of the PS blends (calculated from eq 2) increase slowly with decreasing χ. Both the fibril diameter D and fibril spacing D_0 are shown in Figure 6. These values will be used later to estimate the microscopic parameters of a load-bearing craze fibril.

The median strains for crazing ϵ_c, local fibril breakdown ϵ_b, and catastrophic fracture ϵ_f of the blends (2000 + 1 800 000) are shown in parts a and b of Figure 7 for the

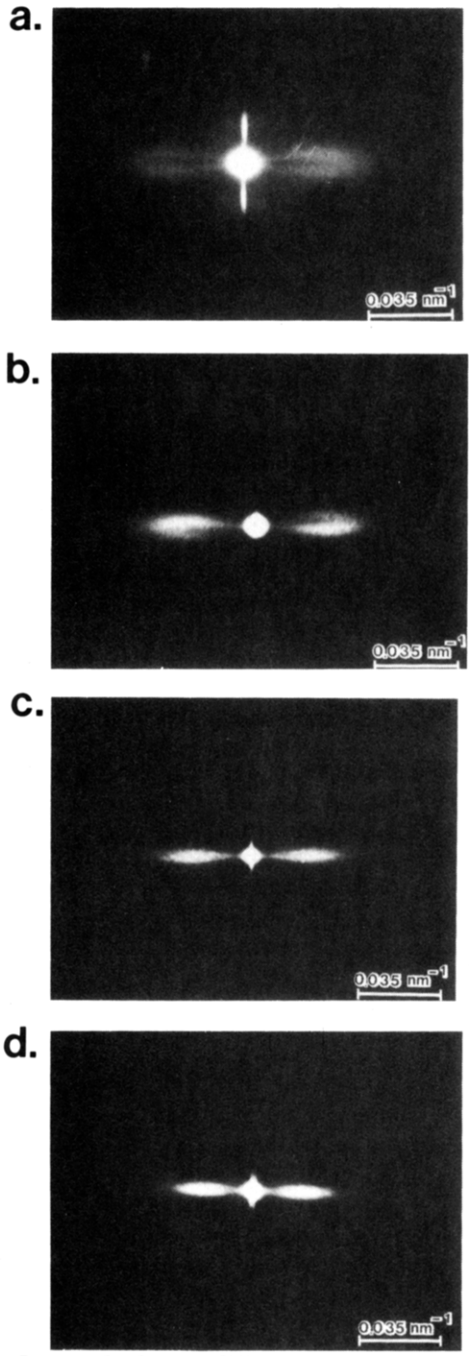

Figure 4. Low-angle electron diffraction patterns for the crazes grown from a "crack tip" in the PS blends (2000 + 1 800 000) with (a) $\chi = 1.0$, (b) $\chi = 0.7$, (c) $\chi = 0.5$, and (d) $\chi = 0.4$.

unfiltered and filtered specimens, respectively. A slower strain rate, 5×10^{-7} s^{-1}, was used for the unfiltered specimens than that, 3×10^{-6} s^{-1}, used for the "ultraclean" specimens. For both the unfiltered and "ultraclean" samples, the behaviors of the strains ϵ_c, ϵ_b, and ϵ_f are quite similar. The crazing strain ϵ_c is approximately 0.7% and is independent of χ within experimental error. The breakdown strain ϵ_b and fracture strain ϵ_f decrease approximately linearly with χ down to $\chi = 0.5$ and approach the crazing strain ϵ_c at $\chi = 0.3$. In this highly diluted blend craze breakdown occurs immediately following craze formation. Note that the craze fibril stability vanishes at a χ well above the overlap concentration, $\approx 8 \times 10^{-4}$ for 1 800 000 molecular weight PS. While there is a large diluent effect on craze fibril stability, the high molecular weight chains are still entangled when the fibril stability has dropped to zero.

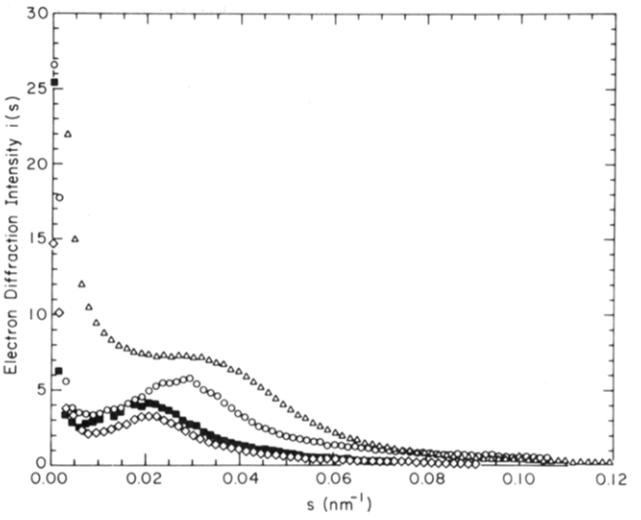

Figure 5. Slit-smeared intensity vs. the magnitude of the scattering vector s parallel to the craze length for the LAED patterns in Figure 4: (△) $\chi = 1.0$; (○) $\chi = 0.7$; (■) $\chi = 0.5$; (◇) $\chi = 0.4$.

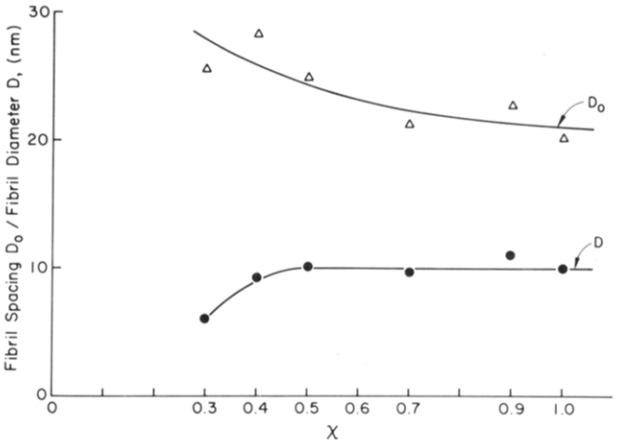

Figure 6. Average fibril diameter D (●) and fibril spacing D_0 (△) vs. the high molecular weight fraction χ in the PS blends (2000 + 1 800 000). The data are derived from a Porod analysis of the LAED pattern, except the values for $\chi = 0.3$, which were obtained from direct measurements from TEM images.

Fibril breakdown always occurs at the craze–bulk polymer interface, forming a pear-drop-shaped cavity[6,9] connected to the interface. In the unfiltered samples, craze fibrils break down preferentially at the dust inclusions whereas in the "ultraclean" films no foreign particle inclusions can be identified at most of the breakdown sites. The ϵ_b and ϵ_f values for the crazes in the "ultraclean" films are higher than those in the unfiltered films, even though a higher strain rate was used for the filtered samples, emphasizing the conclusion of our previous study[9] that the presence of dust strongly decreases the craze fibril stability.

The craze fibril stability has been measured previously for monodisperse PS's with molecular weight M = 37 000–2 000 000 in both the "ultraclean" and unfiltered specimens using the same strain rates.[9] The median strain to craze ϵ_c is constant with molecular weight M in both the unfiltered and filtered specimens. For unfiltered specimens, the median strain for local fibril breakdown ϵ_b and the median strain for catastrophic fracture ϵ_f increase rapidly with M in the region 50 000–200 000 and level off for higher molecular weight, whereas for the "ultraclean" specimens the median strains (ϵ_b and ϵ_f) manifest a similar sharp increase between M = 50 000 and M = 200 000 and then increase approximately linearly with the logarithm of molecular weight. The values of ϵ_b and ϵ_f for the

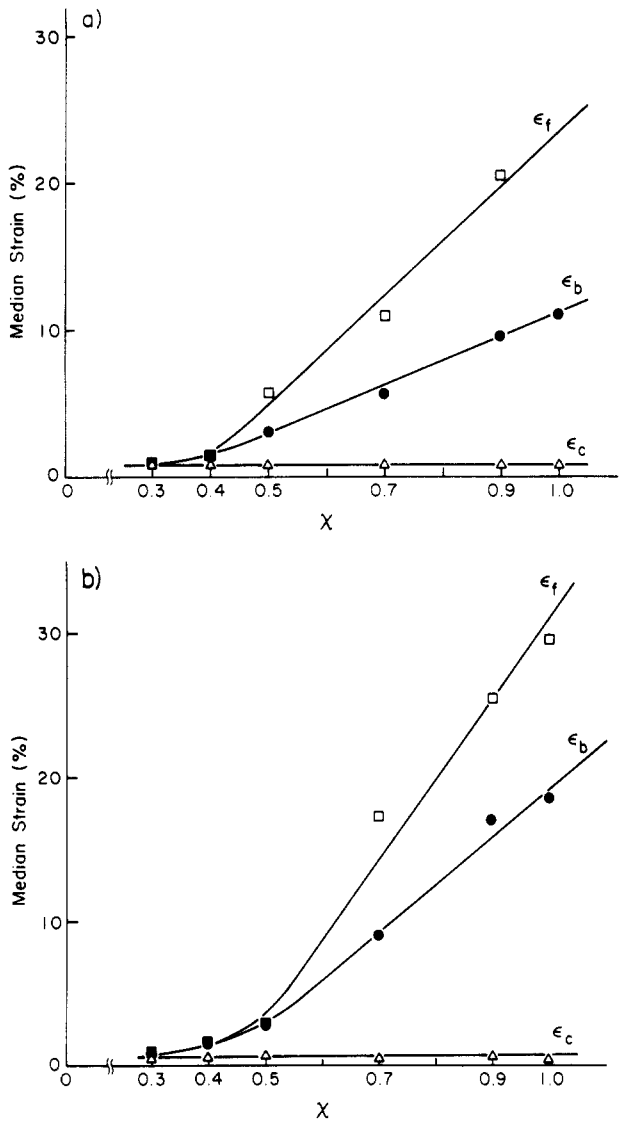

Figure 7. Median strains for crazing ϵ_c (△), fibril breakdown ϵ_b (●), and catastrophic fracture ϵ_f (□) of the crazes in the PS blends (2000 + 1 800 000) for (a) unfiltered specimens (strain rate = 5×10^{-7} s^{-1}) and (b) "ultraclean" specimens (strain rate = 3×10^{-6} s^{-1}). In each case χ is the high molecular weight fraction in the blend.

"ultraclean" specimens are significantly higher than the values measured for the unfiltered specimens.

In our previous study[9] of crazes in monodisperse PS's the statistics for the plastic strain ϵ_p at craze fibril breakdown were found to follow a Weibull distribution.[22] This distribution is given by

$$p(\epsilon_p) = 1 - \exp[-(V_0/V_b)(\epsilon_p/\epsilon_W)^\rho] \quad (4)$$

where the Weibull scale parameter ϵ_W is an alternate measure of fibril stability, the Weibull modulus ρ is a measure of the breadth of the distribution of fibril stability, and V_0 and V_b are the initial volume of a film square and a reference volume, respectively. These Weibull parameters have been obtained for each $\chi \geq 0.5$ in the blends (2000 + 1 800 000) using methodology described in our earlier work.[9] The blends $\chi = 0.3$ and 0.4 were too brittle, unfortunately, to allow data for a Weibull analysis to be acquired.

The behavior of the scale parameter ϵ_W vs. χ resembles that of our measure of fibril stability ($\epsilon_b - \epsilon_c$) for both the filtered and unfiltered specimens. The modulus ρ (high ρ's produce narrower distributions) is approximately equal to 4 for all the "ultraclean" blends. This value is close to the value of $\rho \approx 5$, found previously for monodisperse PS's.[9]

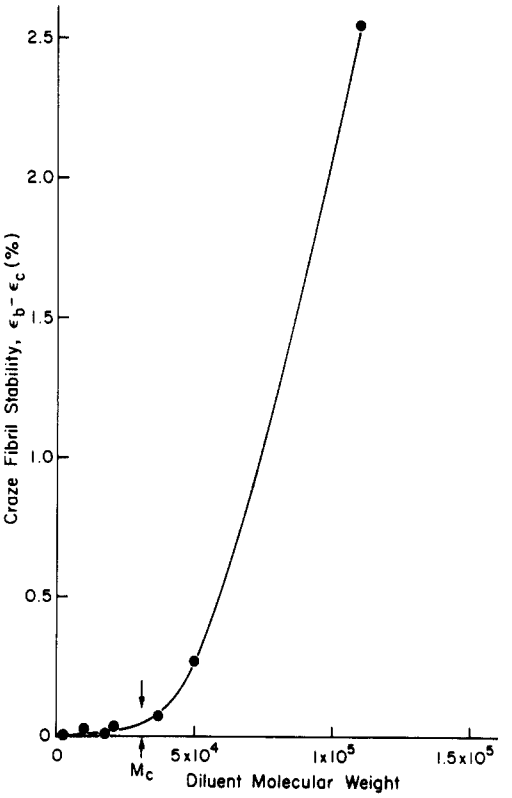

Figure 8. Effect of the diluent molecular weight in blends with 1 800 000 molecular weight PS on craze fibril stability ($\epsilon_b - \epsilon_c$) for a 1 800 000 molecular weight fraction $\chi = 0.3$. The samples were unfiltered and the strain rate was 5×10^{-7} s^{-1}. M_c ($\approx 2M_e$) is the critical molecular weight for entanglement effects on the zero-shear-rate viscosity.

The effects of the molecular weight of the diluent have been briefly examined. Polystyrene of each of the molecular weights 2000, 10 000, 17 500, 20 400, 37 000, 50 000, and 110 000 was used as the diluent for the 1 800 000 molecular weight PS in blends with $\chi = 0.3$, and the fibril stability for such blends was measured. As shown in Figure 8, the value of ($\epsilon_b - \epsilon_c$) of the crazes in the blends increases sharply for $M > 37\,000$ while for the other very low molecular weight diluents it remains very close to zero. At $\chi = 0.5$ and 0.7 the craze microstructures of the blends (2000 + 1 800 000) and (20 400 + 1 800 000) (at the same strain $\epsilon = 2\%$) were compared. The fibril diameter and the fibril spacing in these blends with different diluent molecular weight are approximately the same at the same χ.

A 600 molecular weight PS, which is a liquid at room temperature, was also used as the diluent for 1 800 000 molecular weight PS. For $\chi \leq 0.5$, the 600 molecular weight PS strongly depresses the glass transition temperature of the 1 800 000 molecular weight PS. For this reason the diluent effects of this very low molecular weight species are different from those of the other, higher molecular weight, diluents reported above. At room temperature these films can be uniformly deformed up to a very high strain without the formation of crazes or local deformation zones even in the presence of a starter crack. The reason for this behavior lies in the plasticization effect of the 600 molecular weight PS. For example, the film of $\chi = 0.5$ has a calculated T_g of 8 °C.[23] The rubbery film can be deformed in tension to a strain higher than 27%, beyond the strain at which the copper grid breaks. However, if the ambient temperature is lowered by plunging

the film into a cold environment filled with liquid nitrogen vapor for 3–5 min, crazes can form and break down under applied tensile stress. These crazes formed at low temperature quickly undergo fibril coalescence when heated to room temperature, resulting in much larger fibril dimensions.[13] Craze breakdown again always occurs at the craze–bulk polymer interface and the voids resemble those observed in the other PS's. For the 600 molecular weight PS blends with $\chi = 0.7$ and 0.9, crazes can form at room temperature. The crazing strain ϵ_c, however, increases to 2.1% for $\chi = 0.7$, compared to the normal value of 0.7%. This increase in the crazing strain ϵ_c in the blend may be due to the decrease in the modulus of the bulk polymer with plasticization so that a higher strain is needed in order to reach the critical stress required for crazing. All the crazes have a much coarser fibril structure than those in the 2000 molecular weight PS blends, presumably due to the lower crazing stress and the high fibril coalescence rate. The fibril stability of the crazes in the 600 molecular weight PS blends is extremely high. For example, the value of $(\epsilon_b - \epsilon_c)$ is 23.5% for $\chi = 0.7$, compared to 4.1% for the blend (2000 + 1 800 000) with the same dilution. Since D_0 is much larger, the probability of survival q of each entangled strand in such craze fibrils will be higher as we discuss later. The higher q value, as well as the lower fibrillation stress of the plasticized PS, is believed primarily responsible for this increase in the fibril stability of the 600 molecular weight PS blend.

The equation[23] $T_g = (100 - (1 \times 10^5)/M_n)$ °C was used to calculate the T_g of the PS blends. Also, a series of measurements of the T_g of the blends (2000 + 1 800 000) was made with a differential scanning calorimeter (DSC). A single and well-defined T_g was found for each PS blend. The measured results generally agree with the equation for the blends in the range $0.3 \leq \chi \leq 1.0$, although for 2000 molecular weight monodisperse PS the measured T_g is about 13 °C higher than that calculated from the equation. In the blends (2000 + 1 800 000), T_g decreases linearly with χ, from 100 °C at $\chi = 1.0$ to 67 °C for $\chi = 0.3$. This depression of T_g may be responsible for the increase of the fibril spacing D_0 in the blends. The decrease in T_g also implies a higher chain mobility, which in turn may explain partially the much larger measured values for fibril extension ratio λ_{craze} than the predicted values λ_{max}, which assume no entanglement loss. However, the precise effects of this T_g depression on craze microstructure are not yet understood. In the extreme case of the blends (600 + 1 800 000), the calculated T_g's for various blends are 8 °C ($\chi = 0.5$), 23 °C ($\chi = 0.7$), and 41 °C ($\chi = 0.9$), which are qualitatively consistent with the observed deformation behaviors.

Discussion

An attempt was made to correlate the fibril stability $(\epsilon_b - \epsilon_c)$ for the monodisperse PS's and the PS blends by using the number-average, the viscosity-average, and the weight-average molecular weights M_n, M_v, and M_w. Parts a and b of Figure 9 show the plots of $(\epsilon_b - \epsilon_c)$ vs. average molecular weights for the unfiltered and "ultraclean" specimens. Obviously none of the average molecular weights can allow one to predict the values of $(\epsilon_b - \epsilon_c)$ for the blends from those of the monodisperse polymers.

From the craze microstructural parameters, however, we can calculate the mean number of effectively entangled strands n_e in each craze fibril, which is given as[4,8]

$$n_e = qn_0 \tag{5}$$

where q is the probability that a given entangled strand does not undergo chain scission during fibrillation and n_0

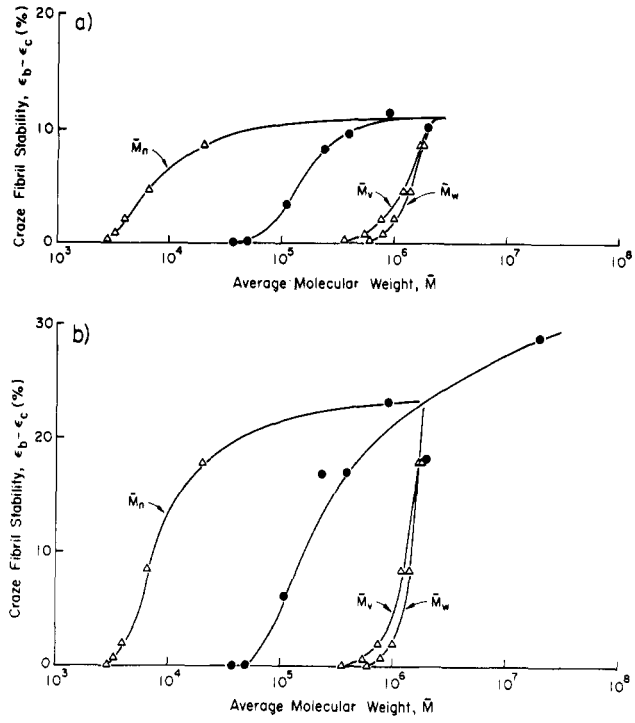

Figure 9. Craze fibril stability $(\epsilon_b - \epsilon_c)$ vs. the number-average molecular weight M_n, the weight-average molecular weight M_w, and the viscosity-average molecular weight M_v for (a) unfiltered specimens (strain rate = 5×10^{-7} s^{-1}) and (b) "ultraclean" specimens (strain rate = 3×10^{-6} s^{-1}): (●) monodisperse PS; (△) (2000 + 1 800 000) PS blends.

is the total number of entangled strands in the undeformed "phantom fibril" from which a craze fibril is drawn. The probability q can be estimated by using Gaussian statistics of a random coil[24] or by geometrical statistics in which q is given as[8]

$$q = 1 - (d/D_0) + B(d/D_0)^m \qquad \text{for } D_0/d > 1 \tag{6a}$$

$$q = B(D_0/d)^m \qquad \text{for } D_0/d < 1 \tag{6b}$$

where $B = 0.155$ and $m = 3.23$. Both methods yield a similar result, $q \approx 0.50$ for undiluted PS. The value of n_0 is given by

$$n_0 = \pi d\nu\chi D_0^2(1 - M_e/M_n)/8 \tag{7}$$

where ν is the entanglement density calculated from the shear modulus $G_N°$ at the rubbery plateau for PS and M_n is the number-average molecular weight of the long-chain species in the bulk polymer blend. The factor $(1 - M_e/M_n)$ is the correction for ν for the finite chain lengths.[25] For diluted networks the value of q calculated from eq 6 decreases approximately linearly as the high molecular weight concentration χ decreases. While the initial number of entangled strands n_0 in each fibril is approximately independent of χ ($n_0 \approx 52$), the mean number of effectively entangled chains n_e decreases approximately linearly with decreasing concentration of high molecular weight chains because of the decrease in q. The values of d, ν, D_0, q, n_0, and n_e for each blend are listed in Table II.

Figure 10 shows that the fibril stability data for the crazes in both the monodisperse molecular weight PS's and the PS blends fall on a single curve when they are plotted against n_e. The value of $(\epsilon_b - \epsilon_c)$ rises almost exponentially with n_e. If dust particles are present, the values of $(\epsilon_b - \epsilon_c)$ are decreased but the shape of the curve (and the good correlation with n_e) remains unchanged.

In our earlier work[9] we related the Weibull modulus and scale parameters, ρ and ϵ_W, respectively, to the process of

Table II
Parameters for the Crazes in the Diluted Polystyrenes

χ (1 800 000 wt fract)	1.0	0.9	0.7	0.5	0.4	0.3
d, nm	9.6	10.1	11.5	13.6	15.2	17.5
ν, $\times 10^{25}$ m^{-3}	3.27	2.94	2.29	1.63	1.31	0.98
D_0, nm (smoothed)	21.2	21.4	22.1	24.5	26.4	28.9
q	0.56	0.56	0.50	0.47	0.45	0.41
n_0	55	53	50	52	53	52
n_e	30.8	29.5	26.5	24.2	23.0	22.6

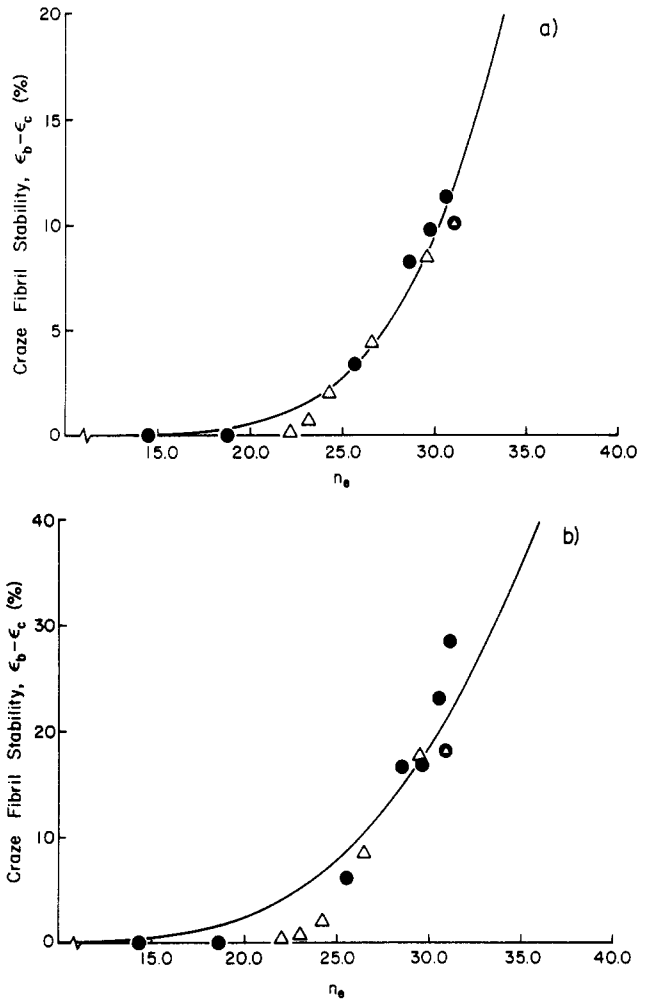

Figure 10. Fibril stability ($\epsilon_b - \epsilon_c$) vs. the number n_e of effective entangled strands in a fibril for the crazes in the PS blends (2000 + 1 800 000). The solid curves represent the theory (eq 8): (a) unfiltered specimens (strain rate = 5×10^{-7} s^{-1}); (b) "ultraclean" specimens (strain rate = 3×10^{-6} s^{-1}); (●) monodisperse PS; (△) (2000 + 1 800 000) PS blends.

fibril formation and breakdown. Two random processes were involved, namely strand scission with probability (1 − q) in the formation of the fibril, and strand disentanglement with probability ξ during drawing in the active zone. Under these processes the strands were treated as independent. Thus during fibril formation the original n_0 entangled strands were reduced to a random number N_d following the binomial distribution with parameters n_0 and $q(1 - \xi)$. Fibril breakdown was assumed to result when $N_d = 0$. This analysis led to an approximately exponential dependence of the fibril stability ($\epsilon_b - \epsilon_c$) on n_e given by[9]

$$\epsilon_b - \epsilon_c = \exp[n_e(1 - \xi(\sigma_0))/\rho][(\mathbf{n}_f V_0)^{-1}(\lambda - 1)\rho \ln 2]^{1/\rho} \quad (8)$$

where $\xi(\sigma_0)$ is the strand disentanglement probability at the drawing stress σ_0 which corresponds to $\epsilon_p = 1$ and $\mathbf{n}_f$ is the number of fibril elements formed from a unit risk volume V_0. All the parameters in eq 8 except $\xi(\sigma_0)$ could

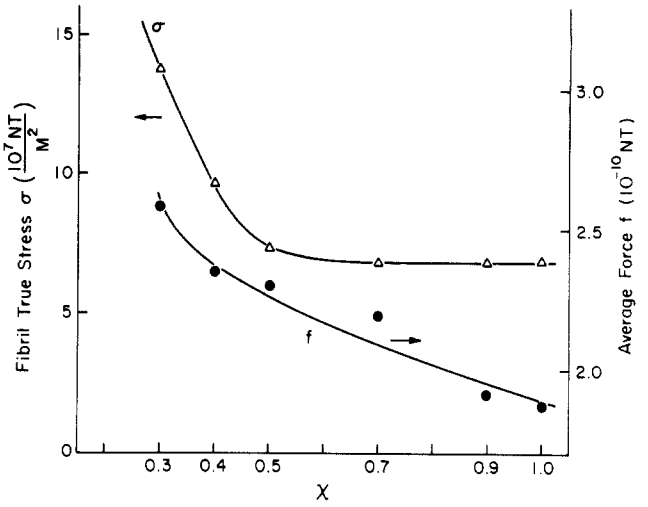

Figure 11. Fibril true stress σ (△) and the average force f (●) on each entangled strand in the drawn fibrils vs. χ, the high molecular weight fraction in the PS (2000 + 1 800 000) blends.

be estimated as described previously;[9] $\xi(\sigma_0)$ was then adjusted to produce the best fit of eq 8 to the data shown by the solid lines in Figure 10. The values of $\xi(\sigma_0)$ thus determined are 0.51 for the "ultraclean" films at a strain rate of 3×10^{-6} and 0.48 for the unfiltered films at a strain rate of 5×10^{-7} s^{-1}. A somewhat higher $\xi(\sigma_0)$ (but still <1) seems necessary to describe the fibril breakdown in the "ultraclean" blends with low n_e's.[9] That the disentanglement probability increases with decreasing molecular weight or increasing dilution seems reasonable. From the comparison between the two sets of data of PS blends and monodisperse PS's, however, the experimental evidence is unequivocal that craze fibril stability is controlled by the mean number of effectively entangled strands n_e in each fibril, independent of the details of the microscopic model for this control.

We can check one more detail of our molecular model, namely the assumption that even a few entangled strands are sufficient to prevent fibril failure. It is evident that a lower n_e would also result in a higher average force on each strand making up a fibril in the active zone, and this force alone might be sufficient to cause fibril breakdown. To show that this is not likely we have estimated from our present data the true stress σ on each fibril and the average force f on each surviving strand. The force on each entangled strand in the fibril, f, can be calculated from the equation[4]

$$f = \pi D_0^2 S/(4n_e) \quad (9)$$

where S is the craze surface stress, given as[4]

$$S = 8\Gamma/D_0\beta \quad (10)$$

in which β is a geometric constant on the order unity and Γ is the surface energy of craze fibrils.[26] The fibril true stress, σ, can be obtained from[4]

$$\sigma = S\lambda_{craze} \quad (11)$$

The calculated values of f and σ of the crazes in the PS blends (2000 + 1 800 000) are shown in Figure 11. As the high molecular weight concentration χ and the effective number of entangled strands n_e decrease, the true stress σ is constant in the region $0.5 \leq \chi \leq 1.0$ and rises sharply for $\chi < 0.5$. This sharp increase in σ for $\chi < 0.5$ reflects a similar increase in the fibril draw ratio λ_{craze}. On the other hand, the average force f per strand increases continuously from 1.9×10^{-10} N at $\chi = 1.0$ to 2.6×10^{-10} N at $\chi = 0.3$. Even at the lowest value of χ, where the fibril stability has all but vanished, the force per strand is over

an order of magnitude smaller than the lowest theoretical (3×10^{-9} N)[4,8] and experimental (6×10^{-9} N)[27,28] estimates of the force required to break a PS chain.

The low molecular weight species ($M < 37\,000$) in the high and low molecular weight PS blend dilutes the entanglement network of the long-chain species. Because the diluent molecules ($M < 37\,000$) are too short to form any effective entanglements, the molecular weight M_e between the neighboring entanglements in the blend becomes larger as the diluent concentration increases, causing a marked decline in the fibril stability and important changes in the fibril structure. The predicted value of λ_{max} from the entanglement network model has proven to be a reliable reference for the true fibril draw ratio λ_{craze} of the crazes of relatively high toughness ($0.5 \leq \chi \leq 1.0$). The much higher value of λ_{craze} than λ_{max} in the blends $\chi = 0.3$ and $\chi = 0.4$ is believed due to the even higher entanglement loss in these brittle crazes.

Finally, there are some questions unanswered. For example, what is happening on a molecular scale when the craze fibril spacing D_0 increases linearly as the diluent concentration is increased but the craze fibril diameter D stays virtually constant? Also, why is the total number of entangled strands n_0 in each fibril essentially constant before crazing regardless of the dilution? The answer to these questions may help us to understand the response of the entanglement network in the glass to deformation and therefore provide insight into fundamental polymer mechanical behavior.

Conclusions

1. The low molecular weight component ($2000 \leq M \leq 37\,000$) in a blend of high and low molecular weight PS dilutes the entanglement network of the high molecular weight species. Craze fibril structure and stability are modified due to the decrease in the entanglement density. The predicted λ_{max} for a strand of the diluted entanglement network is a useful reference for the fibril extension ratio λ_{craze}.

2. In the diluted PS blends ($2000 + 1\,800\,000$), the average craze fibril diameter D is constant with χ down to $\chi = 0.4$ and decreases only slightly at $\chi = 0.3$, while the average fibril spacing D_0 increases modestly as χ decreases.

3. Craze fibril stability decreases almost linearly with decreasing χ until for $\chi < 0.3$ the crazes are so fragile that the craze fibril stability approaches zero.

4. Craze fibril stability increases approximately exponentially with the mean number n_e of effectively entangled strands in each craze fibril in both the diluted PS blends and monodisperse PS's.

5. Craze fibril breakdown follows Weibull statistics in the diluted PS blends as it does in the monodisperse PS's. A model of craze fibril breakdown based on these statistics predicts the increase in fibril stability with n_e.

Acknowledgment. We gratefully acknowledge primary financial support by the Cornell Materials Science Center for E.J.K., C.C.K., and S.L.P. as well as the use of the facilities of the Cornell Materials Science Center, which is funded by the NSF DMR-MRL program. A.C.-M.Y. was supported by a grant from the U.S. Army Research Office, Durham, NC. The use of the clean room facilities of NRRFSS for producing the ultraclean films is gratefully acknowledged.

Registry No. PS (homopolymer), 9003-53-6.

References and Notes

(1) Rabinowitz, S.; Beardmore, P. *CRC Rev. Macromol. Sci.* **1972**, *1*, 1.
(2) Kambour, R. P. *J. Polym. Sci., Part D* **1973**, *7*, 1.
(3) Gent, A. N. *AMD [Symp. Ser.] (Am. Soc. Mech. Eng.)* **1976**, *19*, 55.
(4) Kramer, E. J. *Adv. Polym. Sci.* **1983**, *52/53*, 1.
(5) Lauterwasser, B. D.; Kramer, E. J. *Philos. Mag.* **1979**, *A39*, 469.
(6) Beahan, P.; Bevis, M.; Hull, D. *Proc. R. Soc. London, Ser. A* **1975**, *343*, 525.
(7) Doyle, M. J.; Maranci, A.; Orowan, E.; Stork, S. T. *Proc. R. Soc. London, Ser. A* **1972**, *329*, 135.
(8) Kramer, E. J. *Polym. Eng. Sci.* **1984**, *24*, 761.
(9) Yang, A. C.-M.; Kramer, E. J.; Kuo, C. C.; Phoenix, S. L. *Macromolecules*, preceding paper in this issue.
(10) Donald, A. M.; Kramer, E. J. *Polymer* **1982**, *23*, 461.
(11) Lauterwasser, B. D. Ph.D. Thesis, Cornell University, 1979.
(12) Donald, A. M.; Kramer, E. J. *J. Mater. Sci.* **1981**, *16*, 2967.
(13) Yang, A. C.-M.; Kramer, E. J. *J. Polym. Sci., Polym. Phys. Ed.* **1985**, *23*, 1353.
(14) Brown, H. R. *J. Polym. Sci., Polym. Phys. Ed.* **1983**, *21*, 483.
(15) Paredes, E.; Fischer, E. W. *Makromol. Chem.* **1979**, *180*, 2707.
(16) Brown, H. R.; Kramer, E. J. *J. Macromol. Sci., Phys.* **1981**, *B19*, 487.
(17) Porod, G. *Kolloid Z.* **1951**, *124*, 83; **1952**, *125*, 109.
(18) We are aware that treating entanglements as localized (transient) cross-links does not fully describe the viscoelastic properties of the melt; other models (the tube model, for example) seem superior there. Nevertheless in the glass, where reptation times are long, a network model of the entangled chains still appears appropriate to describe large-strain behavior.
(19) Donald, A. M.; Kramer, E. J. *J. Polym. Sci., Polym. Phys. Ed.* **1982**, *20*, 899.
(20) de Gennes, P.-G. *Scaling Concepts in Polymer Physics*; Cornell University: Ithaca, NY, 1979.
(21) Graessley, W. W. *Polymer* **1980**, *21*, 258.
(22) Weibull, W. *J. Appl. Mech.* **1951**, *18*, 293.
(23) Fox, T. G.; Flory, P. J. *J. Polym. Sci.* **1954**, *14*, 315.
(24) Kuo, C. C.; Phoenix, S. L.; Kramer, E. J. *J. Mater. Sci. Lett.* **1985**, *4*, 459.
(25) In making this chain-end correction we have assumed that two initial chain ends have the same effect as one chain scission during fibril formation. Since we assume that each scission removes one, and only one, strand from the network, the correction factor is $(1 - M_e/M_n)$, rather than the usual $(1 - 2M_c/M_n)$ for a randomly cross-linked network (Flory, P. J. *Principles of Polymer Chemistry*; Cornell University: Ithaca, NY, 1953).
(26) The surface energy Γ of craze fibrils can be explicitly written as[4,8] $\Gamma = \gamma + d\nu_e U/4$. In this expression, γ is the van der Waals surface energy and U is the energy needed to break a chain. We have assumed that chain scission takes full responsibility for all the geometric necessary entanglement loss from fibrillation, which might be the upper bound of the actual case. A value of 0.04 J/m^2 is used for γ, and 6×10^{-19} J for U.
(27) Odell, J.; Keller, A.; Miles, M. J. *Polym. Commun.* **1983**, *24*, 7.
(28) Merrill, E. W.; Horn, A. F. *Polym. Commun.* **1984**, *25*, 144.